Li, X.-M., & Krakow, J. S. (1988) *J. Biol. Chem. 263*, 3448-3453.
Lisitsyn, N. A., Monastyrskaya, G. S., & Sverdlov, E. D. (1988) *Eur. J. Biochem. 177*, 363-369.
Liu-Johnson, H.-N., Gartenberg, M. R., & Crothers, D. M. (1986) *Cell 47*, 995-1005.
Lowe, P. A., Hager, D. A., & Burgess, R. R. (1979) *Biochemistry 18*, 1344-1352.
Majors, S. (1975) *Nature 256*, 672-674.
Malan, T. P., Kolb, A., Buc, H., & McClure, W. R. (1984) *J. Mol. Biol. 180*, 881-909.
McClure, W. R. (1980) *Proc. Natl. Acad. Sci. U.S.A. 77*, 5634-5638.
Park, C. S., Hillel, H., & Wu, C.-W. (1982) *J. Biol. Chem. 257*, 6944-6949.
Peattie, D., & Gilbert, W. (1980) *Proc. Natl. Acad. Sci. U.S.A. 77*, 4679-4682.
Pinkney, M., & Hogget, J. G. (1988) *Biochem. J. 250*, 897-902.
Ren, Y. L., Garges, S., Adhya, S., & Krakow, J. S. (1988) *Proc. Natl. Acad. Sci. U.S.A. 85*, 4138-4142.
Reznikoff, W. S., Siegele, D. A., Cowing, D. W., & Gross, C. A. (1985) *Annu. Rev. Genet. 19*, 355-387.
Riftina, F., DeFalco, E., & Krakow, J. S. (1989) *Biochemistry 28*, 3299-3305.
Rockwell, P., & Krakow, J. S. (1985) *Biochemistry 24*, 3240-3245.
Rockwell, P., & Krakow, J. S. (1988) *Biochemistry 27*, 3512-3520.
Spassky, A., Kirkegaard, K., & Buc, H. (1985) *Biochemistry 24*, 2723-2731.
Stackhouse, T. M., & Meares, C. F. (1988) *Biochemistry 27*, 3038-3045.
Straney, D. C., & Crothers, D. M. (1987) *J. Mol. Biol. 193*, 279-292.
Straney, D. C., Straney, S. B., & Crothers, D. M. (1989) *J. Mol. Biol. 206*, 41-57.
Wu, H.-M. & Crothers, D. M. (1984) *Nature 308*, 509-513.

Effect of Base-Pair Sequence on the Conformations and Thermally Induced Transitions in Oligodeoxyribonucleotides Containing Only AT Base Pairs†

Elizabeth T. Zuo,‡ Farial A. Tanious,‡ W. David Wilson,*,‡ Gerald Zon,§ Guo-shen Tan,∥ and Roger M. Wartell*,∥

Department of Chemistry and Laboratory for Microbial and Biochemical Sciences, Georgia State University, Atlanta, Georgia 30303, Applied Biosystems, Foster City, California 94404, and School of Physics, Georgia Institute of Technology, Atlanta, Georgia 30332

Received August 15, 1989; Revised Manuscript Received December 26, 1989

ABSTRACT: T_m curves, CD spectra, and kinetics results of the self-complementary DNA dodecamers d(A_6T_6), d($A_3T_3A_3T_3$), d($A_2T_2A_2T_2A_2T_2$), d(ATATATATATAT), and d(T_6A_6) demonstrate that the thermal transitions of these oligomers at low salt concentration involve a hairpin intermediate. At high salt concentrations (>0.1 M Na^+) only a duplex to denatured-strand transition appears to occur. The temperature and salt-concentration regions of the transitions are very sequence dependent. Alternating-type AT sequences have a lower duplex stability and a greater tendency to form hairpins than sequences containing more nonalternating AT base pairs. Of the two nonalternating sequences, d(T_6A_6) is significantly less stable than d(A_6T_6). Both oligomers have CD curves that are very similar to the unusual CD spectrum of poly(dA)·poly(dT). The Raman spectra of these two oligomers are also quite similar, but at low temperature, small intensity differences in two backbone modes and three nucleoside vibrations are obtained. The hairpin to duplex transition for the AT dodecamers was examined by salt-jump kinetics measurements. The transition is faster than transitions for palindromic-sequence oligomers containing terminal GC base pairs. Stopped-flow kinetics studies indicate that the transition is second order and has a relatively low activation energy. The reaction rate increases with increasing ionic strength. These results are consistent with a three-step mechanism for the hairpin to duplex reaction: (i) fraying of the hairpin oligomers' terminal base pairs, (ii) a rate-determining bimolecular step involving formation of a cruciform-type intermediate from two hairpin oligomers with open terminal base pairs, and (iii) base-pair migration and formation in the intermediate to give the duplex.

In addition to the well-characterized A, B, and Z double-helical states of DNA (Cantor & Schimmel, 1980; Dickerson et al., 1982; Saenger, 1984; Wells & Harvey, 1987; Blackburn & Gait, 1990), there are nonstandard structures, such as bent, triple-helical, and cruciform-hairpin conformations, which are thought to play important roles in crucial biological processes such as control of gene expression and recombination (Lee et al., 1984; Lyamichev et al., 1986; Moser & Dervan, 1987; Hanvey et al., 1988; Htun & Dahlberg, 1988; Lilley et al., 1988; Petrillo et al., 1988; Chen et al., 1988). Pure AT sequences in double-helical DNA, for example, are known to exhibit significant variations in structure and in interactions with ligands as the sequence on each chain is varied from nonalternating to alternating purine–pyrimidine bases [cf. Saenger (1984) and Yoon et al. (1988)]. Nonalternating AT base pair sequences can lead to curvature of the DNA helix

†This work was supported by NSF Grant DBM-8603566 to W.D.W. and Biomedical Research Support Grant Q5060-3B7 to R.M.W.
‡Georgia State University.
§Applied Biosystems.
∥Georgia Institute of Technology.

0006-2960/90/0429-4446$02.50/0

Chart I

Oligomer Sequence	Abbreviation
d(ATATATATATAT)	$d(AT)_6$
d(AATTAATTAATT)	$d(A_2T_2)_3$
d(AAATTTAAATTT)	$d(A_3T_3)_2$
d(AAAAAATTTTTT)	$d(A_6T_6)$
d(TTTTTTAAAAAA)	$d(T_6A_6)$
d(CGCGAATTCGCG)	Dickerson

axis and have unusual interaction properties and spectra relative to mixed-sequence DNA (Arnott, 1975; Wu & Crothers, 1984; Trifonov, 1985; Marky et al., 1985; Wilson et al., 1985a,b, 1986; Jones et al., 1986; Diekmann, 1987; Nadeau & Crothers, 1989).

Several studies indicate that differences exist between $A_4T_4N_2$ and $T_4A_4N_2$ sequences (Hagerman, 1986; Burkoff & Tullius, 1988; Sarma et al., 1988; Gupta et al., 1988; Haran & Crothers, 1989). Crystallographic studies of oligonucleotides with nonalternating AT base pairs have shown that this sequence can occur with a high propeller twist and a bifurcated hydrogen bond in the major groove between the amino group of A and the *O*4-keto group of a cross-strand T (Nelson et al., 1987; Coll et al., 1987; DiGabriele et al., 1989). A similar bifurcated hydrogen-bond arrangement cannot occur in alternating AT sequences. X-ray crystallographic results with the alternating tetramer pATAT (Viswamitra et al., 1982) led Klug et al. (1979) to propose an "alternating-B" conformation for extended duplex regions of this sequence. In the alternating model the A to T steps have good base stacking and a 33° twist angle while the T to A steps have poor base stacking and a 39° helical twist. This proposal has received support from recent X-ray crystallographic results with d(CGCATATATGCG) (Yoon et al., 1988).

In addition to structural differences, alternating and nonalternating AT sequences in DNA have significantly different interaction properties (Bresloff & Crothers, 1981; Strum, 1982; Chaires, 1983; Marky et al., 1985; Wilson et al., 1985a, 1986; Jones et al., 1986). The mono- and dicationic phenanthridinium probe molecules ethidium and propidium, for example, exhibit very similar thermodynamic parameters in their interaction with alternating AT and GC polymers and with mixed-sequence DNA (Wilson et al., 1985a, 1986). With the nonalternating AT polymer, however, weaker and highly cooperative binding interactions were observed. Binding to the alternating polymers is enthalpy driven while binding to the nonalternating AT polymer is entropy driven (Wilson et al., 1985a). These unusual interaction properties also occur in inverted-repeat dodecamer oligonucleotides with alternating and nonalternating AT sequences (Jones et al., 1986). AT oligomers also exhibit sequence-dependent variations in electrophoretic mobilities (Wilson et al., 1987; Chen et al., 1989).

As part of our continuing investigation of the sequence-dependent differences in structure and properties of AT regions of DNA, we report here an analysis of the conformations and duplex–hairpin–denatured strand transitions of the dodecamers shown in Chart I. All possible inverted-repeat AT dodecamers have been investigated, and each sequence has the potential to form hairpin structures (Scheffler et al., 1968; Lilley et al., 1987; Marky et al., 1983). Circular dichroism and Raman spectroscopy were employed to investigate the sequence-induced conformational variations of the DNA oligomers.

Our results demonstrate that oligomers with alternating purine–pyrimidine base pairs have significantly lower T_m values and greater hairpin-forming tendencies than oligomers with nonalternating base pairs. The behavior is consistent with earlier observations on DNA polymers (Wells et al., 1970; Oliver et al., 1977). Oligomers $d(A_6T_6)$ and $d(T_6A_6)$ show similar CD and Raman spectra at low temperatures; however, small differences are observed in both spectra. The CD spectra of these oligomers differ around 260–270 nm. Raman spectra show intensity differences in two backbone modes and three nucleoside vibrations at 4 °C which are not observed at room temperature. In contrast to the small implied structural differences between the duplex forms of $d(A_6T_6)$ and $d(T_6A_6)$, the thermal stability of $d(T_6A_6)$ is lower than that of $d(A_6T_6)$ by 10–11 °C.

Materials and Methods

Oligonucleotides. The oligonucleotides of Chart I were synthesized and purified, and stock solutions were prepared as previously described (Jones et al., 1986; Wilson et al., 1988). Stock solution concentrations were determined by absorption spectroscopy at 260 nm in PIPES buffer with 0.2 M Na^+ (see below) at 6 °C with the following extinction coefficients: $d(A_6T_6)$, 6000 cm^{-1} M^{-1}; $d(A_3T_3)_2$, 6400 cm^{-1} M^{-1}; $d(A_2T_2)_3$, 6600 cm^{-1} M^{-1}; $d(AT)_6$, 6600 cm^{-1} M^{-1} [determined as previously described (Jones et al., 1986)]. Under these conditions of salt and temperature, the oligonucleotides are in a duplex state as determined by T_m and electrophoresis experiments.

Buffers. Melting, CD, and kinetics experiments were performed in PIPES buffer (0.01 M PIPES, 0.001 M EDTA, pH 7.0, 0.02 M Na^+) adjusted to the desired molarity of Na^+ by the addition of NaCl. In the text we refer to this buffer in terms of Na^+ molarity. Electrophoretic experiments were performed in TBE, TBM, and PIPES buffers. TBE buffer contains 0.1 M Tris, 0.1 M boric acid, and 0.002 M EDTA, pH 8.3; TBM buffer contains 0.1 M Tris, 0.1 M boric acid, and 0.005 M $MgCl_2$, pH 8.3.

UV Spectroscopy. UV spectral analysis and melting experiments were performed on a Cary 2200 or Cary 219 spectrophotometer interfaced to an Apple IIe microcomputer. Up to five cells were monitored and thermostated in a five-position rotatable cell turret. Temperature control was through a Haake PG20 temperature programmer connected to a Haake A81 refrigerated water bath. Temperature was monitored by a Cary 219 thermistor sealed in a reference cuvette in one position of the turret. Other cuvettes had Teflon stoppers, and all were 1-cm path-length quartz cells. Nitrogen gas was passed continuously through the sample compartment of the Cary 219 during low-temperature measurements. Digitized absorbance values were plotted as a function of temperature on the Cary 219 chart recorder and were simultaneously stored by the computer for subsequent plotting and analysis. The computer collected and averaged 10 absorbance readings for each point on the T_m curve to improve signal to noise. T_m measurements were initiated near 0 °C, and the temperature ramp was 0.5 °C/min. Slower heating rates did not affect the experiments within experimental error. For the relatively broad T_m curves obtained for the DNA oligomers, absorbance readings were collected only once per minute, and this typically resulted in more than 100 points for a melting curve and base line. The digitized results were fitted with a nonlinear least-squares fitting program that used sloping base lines in both the low- and high-temperature regions.

Circular Dichroism Measurements. Temperature-dependent CD spectra were obtained with a JASCO 600 spectrophotometer interfaced to an IBM computer. The instrument was operated and data was stored and manipulated with software supplied with the instrument by JASCO. The temperature was controlled by a Fisher refrigerated water bath (Model 90) connected with a thermostated cell holder. All CD spectra were obtained in the low-salt PIPES buffer in 1-cm

path-length cuvettes. The temperature was measured by a Electromedics ITS 600 temperature monitor before and after each CD spectral measurement.

Raman Spectroscopy. Raman spectra of d(A_6T_6) and d(T_6A_6) were obtained with instrumentation previously described (Wartell & Harrell, 1986). An argon ion laser provided 100–120 mW of power at the sample at 514.5 nm. DNA concentrations were about 30 mg/mL in a 0.2 M NaCl solution. Spectra were obtained with the samples at 4 and 25 °C. One spectrum consisted of the sum of four consecutive scans, with each scan collecting data at 2 s/cm^{-1}. Two or three spectra were obtained for each sample condition and averaged. Background curves of spectra were determined with the least-squares curve-fitting procedure of Wartell and Harrell (1986).

Electrophoresis. Electrophoresis was carried out on gels containing 20% polyacrylamide [30:0.8 acrylamide:bis(acrylamide)] under controlled temperature conditions (Maniatis et al., 1975; Frank & Koster, 1979; Wilson et al., 1987). The gels were prepared in a Bio-Rad Protean II gel apparatus using 0.75-mm spacers. Oligomers (20 A_{260} units/mL) were diluted 1:10 with gel-loading buffer (TBE containing 0.05% bromophenol blue plus 8% sucrose) and applied to the gel in 2–6-μL volumes. The temperature was controlled with a Haake A81 circulating water bath. Temperature measurements were made by inserting a thermometer into the buffer reservoir during the experiment. The experiments were conducted at 6–8 mA in TBE and PIPES buffers with no added NaCl and at 10–12 mA in TBM buffer. The electrophoresis was stopped when the bromophenol blue tracking dye had migrated approximately 15 cm. Gels were then stained with propidium iodide for 5 min and photographed under UV light with a Polaroid MP-4 land camera equipped with a Wratten No. 9 filter and Polaroid 665 film.

Kinetics Experiments. We first attempted to monitor the kinetics of the hairpin to duplex equilibrium with a Cary 219 spectrophotometer at 260 nm by rapidly decreasing the temperature in a manner similar to that described by other workers (Scheffler et al., 1968; Xodo et al., 1988a,b). The reactions with these short AT sequence oligomers, however, are fast and have small absorbance changes. It is difficult to distinguish small effects due to final temperature reequilibration from the actual reaction in much of the kinetic region.

Salt-jump kinetic measurements of the hairpin to duplex reaction could be made quite easily with all oligomers with a Hi-Tech SF-51 stopped-flow spectrometer at 260 nm. The HS-1 Datapro software provided with the instrument was used for both data acquisition and analysis. Kinetics results were fitted to both first-order and second-order functions with a nonlinear least-squares routine based on the gradient-expansion method developed by Marquardt. Data acquisition is carried out via a high-speed (>80 kHz) 12-bit analogue to digital converter in a HP-330 computer. Single-wavelength kinetic records of voltage versus time were collected and stored. Typically, five runs were averaged in the computer to improve the signal to noise ratio. The hairpin to duplex reaction was monitored by mixing equal volumes (100 μL) of oligomer in PIPES buffer at the desired temperature and concentration with a buffer of high ionic strength (see Table I). The temperature control was through a Haake A81 refrigerated water bath. The measurements were made in a 1-cm path-length quartz cell at 260 nm as a function of temperature.

Salt-jump experiments were also conducted with a Cary 219 spectrophotometer at 260 nm by mixing equal volumes of PIPES [containing d(A_6T_6) oligomer] with PIPES containing 0.8 M Na^+ at 24 °C in a split-compartment quartz UV cuvette. The cell with the separated solution was first equilibrated at the desired temperature and the absorbance collected. The cell was then inverted to mix the solutions, and the absorbance was collected as a function of time. These experiments were conducted primarily to test the base-line readings obtained in the stopped-flow experiment. The agreement between the two methods was good, but the experimental error in the stopped-flow method was much less.

Results

Characterization of the Transitions. Baldwin and coworkers established several criteria for identification of a hairpin intermediate in the thermal transitions of alternating AT sequence oligomers of varying length (Scheffler et al., 1968, 1970). The duplex to hairpin transition can be detected at low salt concentration, is concentration dependent, and is quite sharp. This transition is followed by a broad hairpin to denatured-strand transition at higher temperatures which is not concentration dependent. The hairpin to duplex transition is much slower and has a higher activation energy than the denatured-strand to hairpin or the denatured-strand to duplex transitions (Scheffler et al., 1968, 1970; Nelson & Tinoco, 1982). Marky et al. (1983) performed a detailed analysis of the duplex–hairpin–denatured transitions for the Dickerson sequence oligomer. As with the pure AT sequence oligomers, T_m curves for the Dickerson sequence at low salt concentration have a sharp duplex to hairpin transition at low temperature followed by a broad hairpin to denatured-strand transition at higher temperature. Results by Wemmer et al. (1985) and Xodo et al. (1988a,b) also demonstrate that self-complementary oligomers with AT central sequences, such as those in Chart I, form hairpin intermediates in their melting transitions at low salt concentration and that at high salt concentration only the duplex to denatured-strand transitions are seen.

Since many physical studies have been conducted with the Dickerson sequence and since its duplex–hairpin–denatured transition behavior is well characterized (Patel et al., 1982; Marky et al., 1983), we included this oligomer in our experiments as a model for characterizing the transitions of the AT oligomers. As indicated above there are several characteristic features that indicate a hairpin intermediate in the thermal transition of a self-complementary oligomer. One characteristic is a sharp transition, for the duplex to hairpin reaction, followed at higher temperatures by a broad transition for the hairpin to denatured-strand transition. Because the two transitions have different salt dependencies, the biphasic behavior disappears at high salt. The slow kinetics of the hairpin to duplex reaction relative to those of the denatured-strand to duplex transition is another key characteristic. In addition to these characteristics, we have also employed two other methods to monitor the occurrence of a hairpin intermediate. The electrophoretic behavior of the duplex, hairpin, and denatured species are different and can be detected by mobility measurements as a function of temperature. We also show that the CD spectral behavior in the 270–280-nm spectral range displays characteristic behavior for transitions with a hairpin intermediate. The molar ellipticity first increases in this spectral region when a hairpin is formed from duplex and then decreases in the hairpin to denatured-strand transition at higher temperature. As expected for the complex equilibria, no isoelliptic points are obtained when the hairpin is an intermediate.

Results for the d(A_6T_6) oligomer are given as examples below, and results for the other oligomers of Chart I are

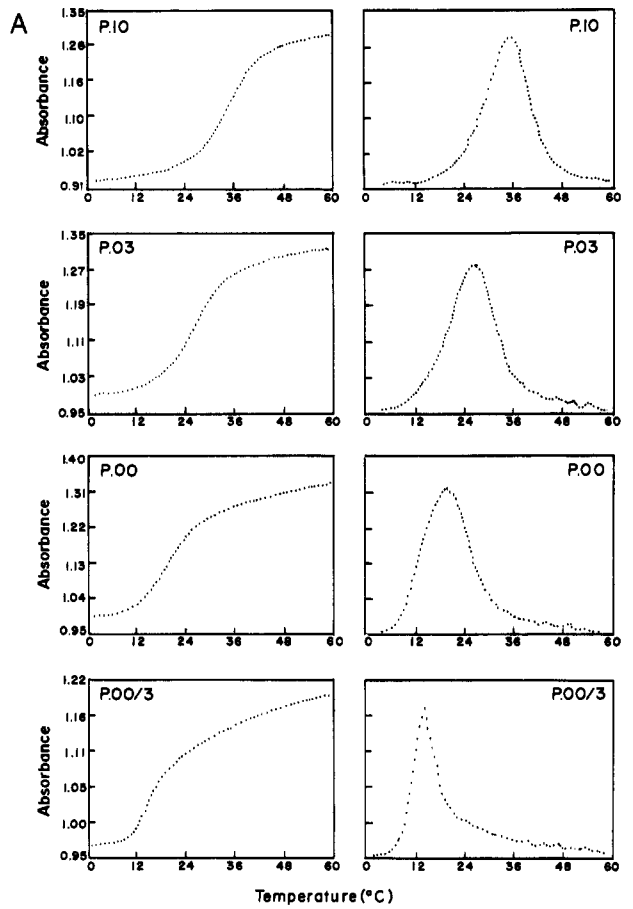

FIGURE 1: (A) Melting curves in different salt concentration buffers for $d(A_6T_6)$. The relative absorbance changes at 260 nm are plotted as a function of temperature (left side) with the corresponding derivative curves (right side). The concentration of oligomer in each experiment was about 0.15 mM in bases. Experiments were conducted in 1-cm path-length cells, and the buffers used were as follows: P.00/3, PIPES diluted by 1/3 with no added salt; P.00, PIPES with no added salt; P.03, PIPES with 0.03 M NaCl; P.10, PIPES with 0.1 M NaCl. (B–E) See supplementary material.

collected in the supplementary material (see paragraph at end of paper regarding supplementary material).

T_m Determinations: Effects of Ionic Strength. Melting curves for the self-complementary oligomers of Chart I display different behavior in the low and high salt concentration regions. The experimental absorbance versus temperature profiles for the $d(A_6T_6)$ oligomer are shown for several salt concentrations in Figure 1 (left side) along with the corresponding derivative curves (right side), and curves for the remaining oligomers are given in Figure 1B–F. The curves are reversible on slow cooling and are reproducible within the error limit of the spectrophotometer. Both the shape of the curve and the temperature at the midpoint (apparent T_m) are dependent on the salt concentration. Melting curves at the lower ionic strengths are biphasic and have sharp transitions for $d(A_6T_6)$, $d(T_6A_6)$, $d(A_3T_3)_2$, and $d(A_2T_2)_3$ at low temperature followed at higher temperatures by broad transitions, characteristic behavior of a hairpin intermediate [cf. Scheffler et al. (1968, 1970), Marky et al. (1983), and Xodo et al. (1988a,b)]. The low-temperature transition was dependent on oligomer concentration while, within experimental error, the upper transition was not, behavior again consistent with a hairpin intermediate. In contrast to the other oligomers, the $d(AT)_6$ oligomer has very broad melting curves at low salt concentration, and biphasic behavior was difficult to detect at the lowest salt concentrations (Figure 1D). Biphasic behavior can, however, be seen in the derivative curves at intermediate ionic strength (from 0.02 to 0.1 M Na^+) where a large absorbance change at high temperature is preceded by a smaller change at low temperature. Electrophoretic and CD results presented below indicate that this oligomer is primarily in a hairpin conformation at low temperature and the broad transition reflects a hairpin to denatured-strand equilibrium.

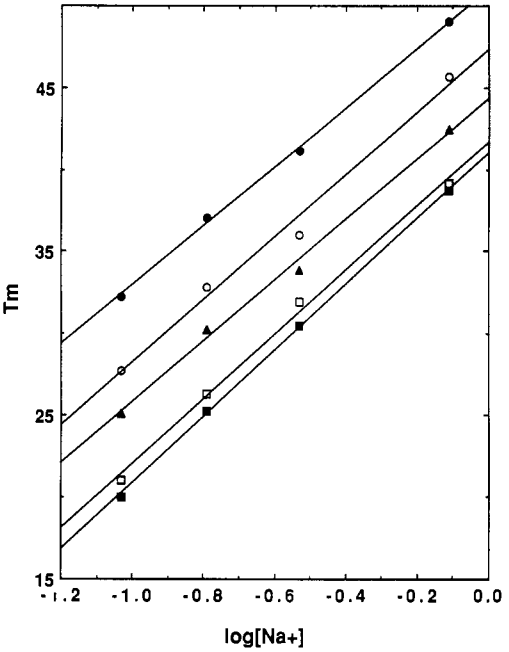

FIGURE 2: Plot of apparent T_m values for the duplex to single-strand transition (determined from the peaks in the derivative plots) versus log (Na^+ activity) for $d(A_6T_6)$ (●), $d(A_3T_3)_2$ (○), $d(A_2T_2)_3$ (▲), $d(AT)_6$ (■), and $d(T_6A_6)$ (□). The concentration of the oligomers in all cases was near 0.15 mM in base pairs.

All of the oligomers exhibited monophasic transitions, characteristic of a duplex to denatured-strand equilibrium, in the higher salt concentration buffers (0.1 M Na^+ and above). Figure 2 shows T_m versus log [Na^+] plots for the melting curve data obtained at Na^+ concentrations from 0.1 to 1.0 M. The monophasic transitions obtained in these solvents are sharp enough for precise T_m determinations. All oligomers have similar slopes (19 ± 1), but their T_m values at a fixed salt concentration are significantly different. $d(A_6T_6)$ has the highest T_m followed by $d(A_3T_3)_2$, $d(A_2T_2)_3$, $d(AT)_6$, and $d(T_6A_6)$.

The T_m values of $d(T_6A_6)$ (Figure 1E) are lower than the T_m values of the other nonalternating sequence, $d(A_6T_6)$, by 10–11 °C from 0.01 to 1.0 M Na^+. The shapes of the $d(T_6A_6)$ melting curves are very similar to the curves for $d(A_6T_6)$ (e.g., Figure 1A,E), and both DNAs have similar slopes of T_m versus log [Na^+] in high salt. Thus, both DNAs appear to undergo a duplex to hairpin to denatured-strand equilibrium at low ionic strength and a duplex to denatured-strand transition at high ionic strength but to have significantly different ranges of thermal stability for the various conformations.

T_m Determinations: Concentration Dependence. To determine the effects of oligomer concentration on the high-salt monophasic transition, the T_m values in 0.4 M Na^+ buffer for the oligomers of Chart I were determined as a function of concentration (not shown). Within experimental error, all oligomers gave linear plots that were fitted with a linear least-squares program to eq 1, where $\Delta S°$ and $\Delta H°$ are the

$$1/T_m = -(R/\Delta H°) \ln C + \Delta S°/\Delta H° \quad (1)$$

entropy and the enthalpy changes for the transition; C is the

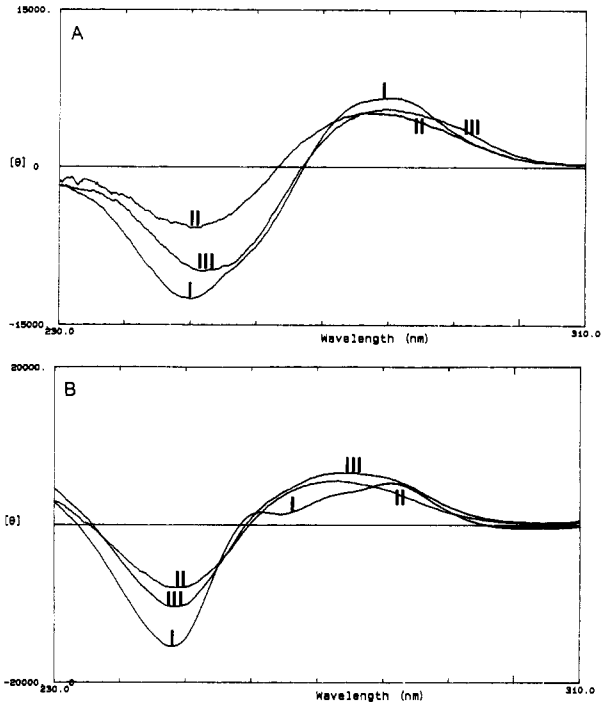

FIGURE 3: Circular dichroism spectra for (A) the Dickerson oligomer and (B) $d(A_6T_6)$. The measurements were conducted in low salt buffer (PIPES with no added NaCl), and the concentration of oligomer was about 0.1 mM in bases in each experiment. Temperatures were adjusted such that in each case curve I shows a spectrum for the duplex conformation, curve II shows a spectrum for the denatured form, and curve III shows a spectrum primarily for the hairpin conformation for each oligomer. (C–F) See supplementary material.

concentration of the oligomers in strands and is equal to K_{eq} at the T_m. In 0.4 M Na^+ buffer all oligomers show only a single transition, which has a significant concentration dependence. This supports the earlier interpretation of a duplex to denatured-strand transition for the high-salt melting curves. The van't Hoff enthalpies determined in this manner are 80 ± 5 kcal/mol for $d(A_6T_6)$, 73 ± 5 kcal/mol for $d(A_3T_3)_2$ and $d(A_2T_2)_3$, and 70 ± 5 kcal/mol for $d(AT)_6$.

The concentration dependence of the T_m for the broad transition for $d(AT)_6$ was also obtained at low salt concentration (not shown). The transition at low ionic strength does *not* have a significant concentration dependence. This is characteristic of a hairpin to denatured-strand conformational change and supports the proposal that $d(AT)_6$ exists primarily in the hairpin conformation at low temperature and low salt concentration. At salt concentrations above 0.1 M Na^+, the oligomer is predominantly in the duplex state at low temperature, and only the duplex to denatured-strand equilibrium is indicated by the transition curves.

Circular Dichroism Spectra. Under low-temperature conditions, the CD spectrum of the Dickerson oligomer (Figure 3A) is typical of a right-handed B-form conformation (Cantor & Schimmel, 1980), and spectral comparisons indicate that all of the AT oligomers of Chart I have a right-handed conformation at low temperature (Figure 3B–F). At low temperature, $d(A_6T_6)$ exhibits an unusual CD spectrum, especially in the longer wavelength region of the positive molar ellipticity (Figure 3B), which is quite similar to the unusual CD spectrum of poly(dA)·poly(dT) (Arnott, 1975). It has two peaks, near 260 and 282 nm, and a shoulder near 273 nm. The Dickerson oligomer (Figure 3A) has only one broad peak centered near 280 nm. The $d(T_6A_6)$ sequence has a CD spectrum (Figure 3F) at low temperature which is similar to the duplex spectrum of $d(A_6T_6)$; however, the crossover point from negative to

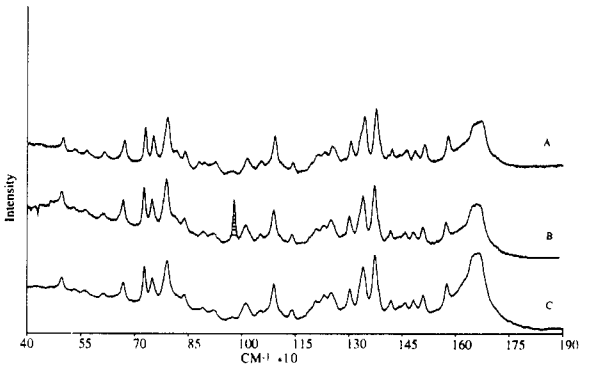

FIGURE 4: Raman spectra of (A) poly(dA)·poly(dT), (B) $d(A_6T_6)$, and (C) $d(T_6A_6)$ obtained at 25 °C in 0.2 M NaCl. The crosshatched peak at 980 cm^{-1} in the $d(A_6T_6)$ spectrum is due to sodium sulfate serving as a frequency marker.

positive molar ellipticity is shifted upward by 10 nm. The oligomers $d(A_3T_3)_2$ (Figure 3C) and $d(A_2T_2)_3$ (Figure 3D) have CD spectra more similar to the Dickerson sequence than to $d(A_6T_6)$. Both oligomers have the band at ~282 nm but not the 262-nm peak, which are characteristic of nonalternating AT sequences.

CD results as a function of temperature provide additional support for hairpin intermediates in the thermal transitions of the AT oligomers at low salt concentration. As the temperature is increased for the oligomer solutions at low salt concentration (Figure 3), there are no isoelliptic points, confirming that multiple species and transitions are present.

Results with the well-characterized Dickerson sequence provide a key for interpreting the AT oligomer spectra. The peak intensity of the negative CD band, which occurs for all species near 250 nm, decreases continuously as the temperature is increased for the Dickerson and AT oligomer sequences. The longer wavelength positive ellipticity region appears to provide a signature for a hairpin intermediate. For the Dickerson sequence (Figure 3A), at conditions that produce the long wavelength region conformation, the highest molar ellipiticity is obtained. In this region the ellipticity increases and then decreases as the temperature is increased. With $d(A_6T_6)$ (Figure 3B) a similar behavior is obtained. The hairpin conformation appears to have greater ellipticity throughout the long-wavelength region. All of the AT oligomers except $d(AT)_6$, which exists predominantly in a hairpin conformation at low temperature and low salt concentration, have intensity increases and then decreases at ~270 nm as the temperature is increased. This behavior is consistent with the formation of a hairpin intermediate in the melting transitions, on the basis of the behavior of the Dickerson sequence.

Raman Spectra. Raman spectroscopy was employed to compare the conformations of $d(A_6T_6)$ and $d(T_6A_6)$ in 0.2 M NaCl at 4 and 25 °C. The low-temperature CD spectra of these DNAs indicate that they are similar but may have small conformational differences. Figure 4 compares the 25 °C spectra of $d(A_6T_6)$ and $d(T_6A_6)$ with the spectrum of poly(dA)·poly(dT). Both oligomers have spectra similar to the polymer. Poly(dA)·poly(dT) adopts a B-family conformation in solution (Thomas & Peticolas, 1984; Wartell & Harrell, 1986) with spectroscopic characteristics indicating tilted base pairs (Edmondson & Johnson, 1985; Nadeau & Crothers, 1989). Background curves of these spectra were similar and were removed by a least-squares curve fitting procedure (Wartell & Harrell, 1986).

A more detailed comparison of the two dodecamers was made with the 1091-cm^{-1} phosphate symmetric stretch mode as an internal standard. Difference spectra from 625 to 1535

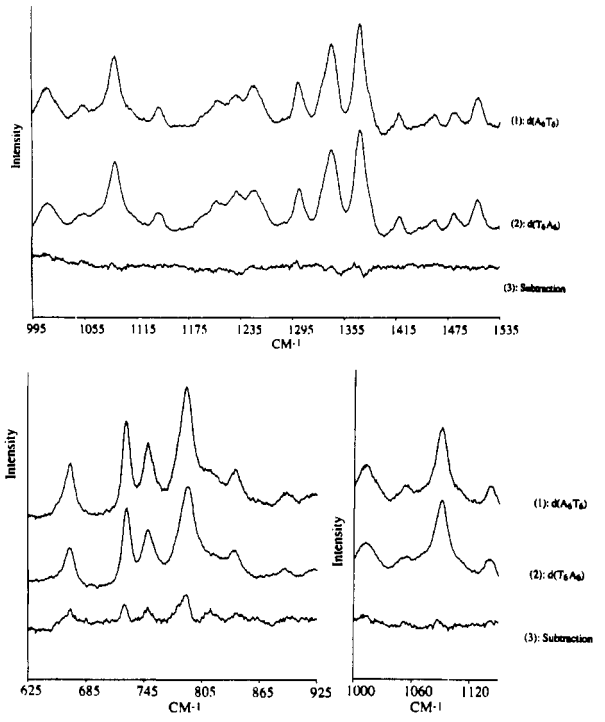

FIGURE 5: Raman spectra of (1) $d(A_6T_6)$ and (2) $d(T_6A_6)$ and the difference spectrum of (1) − (2) obtained at 4 °C.

cm^{-1} are shown in Figure 5 for the 4 °C data. The intensity scale is the same for all panels of the figure. The $d(A_6T_6)$ oligomer has a larger intensity at 790 cm^{-1} than $d(T_6A_6)$. This band is associated with a deoxyribose–phosphate mode and a mode involving in-plane thymine motions (Peticolas et al., 1987; Thomas, 1987; Patapoff et al., 1988). A greater intensity is also seen with $d(A_6T_6)$ at other bands in this region: thymidine bands at 668 and 748 cm^{-1} and the adenine 727-cm^{-1} mode. The backbone mode at 815 cm^{-1} also shows a small intensity difference. In contrast, the region from 1000 to 1500 cm^{-1} shows no significant differences with the possible exception of a frequency shift around the 1370-cm^{-1} thymine mode.

We also compared spectra for the same samples at 25 °C (Figure 6). At this temperature the two spectra are essentially identical, and the differences observed in Figure 5 are not present. These results imply that a small conformational difference exists between the dodecamers at 4 °C that is not detectable at 25 °C.

Electrophoresis. Although the duplex and hairpin conformations are easily resolved in electrophoresis experiments with the Dickerson oligomer and d(GCATATATATGC), every AT oligomer migrated as a single band with temperature-dependent mobility at all temperatures (Figure 7). The observation of a single band indicates that on the time scale of the electrophoresis experiment there is a fast interconversion between duplex and hairpin species of the AT oligomers and the conformations cannot be resolved on electrophoresis gels. On increasing the temperature above the duplex–hairpin transition, only a single band is observed for all of the oligomers, which indicates a fast exchange between hairpin and denatured strands as expected.

At low ionic strength and 5 °C (Figure 7) the Dickerson and d(GCATATATATGC) oligomers are primarily duplex, but weak hairpin bands are visible. Mobilities of the single bands observed for the 5′-A oligomers form a hierarchical order of $d(AT)_6 > d(A_2T_2)_3 > d(A_3T_3)_2 > d(A_6T_6)$. This result indicates a decreasing population of the hairpin species as the sequence changes from alternating to nonalternating

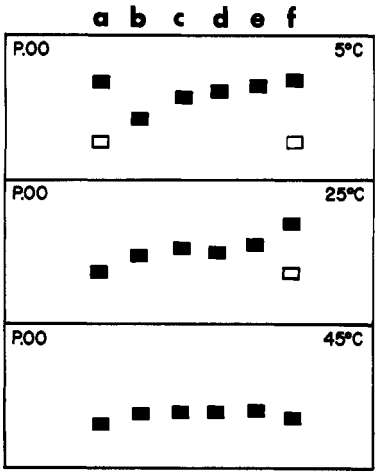

FIGURE 7: Schematic drawing of the electrophoretic profiles for the oligomers of Chart I. The electrophoresis experiments were conducted in P.00 (PIPES with no added salt) as a function of temperature: lane a is for d(GCATATATATGC); lane f is for the Dickerson oligomer; lane b is for $d(AT)_6$; lane c is for $d(A_2T_2)_3$; lane d is for $d(A_3T_3)_2$; lane e is for $d(A_6T_6)$. In the drawing (□) shows the weak bands, and (■) shows the heavy bands.

and supports the conclusions from the melting curve experiments. When the temperature is increased to 25 °C, d(GCATATATATGC) is completely converted to the hairpin conformation while the Dickerson sequence still has a significantly stronger duplex than hairpin band. The mobilities of all AT species have shifted significantly to the single-strand region. At 45 °C (Figure 7) all oligomers contain only single-strand species, which cannot be resolved. The $d(T_6A_6)$ oligomer was analyzed separately (not shown). At low temperature it has a mobility more similar to that of $d(AT)_6$ than to that of $d(A_6T_6)$. By 25 °C it has the same mobility as $d(AT)_6$ in agreement with the T_m results.

Kinetics of the Low-Temperature Transition. A critical test of the existence of a hairpin intermediate in the thermal transitions of the AT oligomers of Chart I is the kinetics of duplex formation relative to the kinetics for oligomers that cannot form hairpins. If a hairpin intermediate is present, the kinetics are slowed by the necessity to open the hairpin, at least partially, before formation of the duplex can be initiated. The kinetics of duplex formation for the AT oligomers were followed at constant temperature by increasing the ionic strength (salt-jump) from low salt concentration to the duplex region of stability in both a Cary 219 and a stopped-flow spectrometer. Kinetic traces for duplex formation with $d(A_6T_6)$, determined by the stopped-flow salt-jump method, are shown in Figure 8 at two different oligomer concentrations. At the lower concentration the results are fitted reasonably well by both first- and second-order functions. At the higher concentration, the signal to noise is improved, and the second-order fit is clearly superior to the first-order fit. As can be seen from the figure, the apparent first-order rate constant varies with oligomer concentration while the second-order rate constant does not change within experimental error, conclusively demonstrating that the reaction is second order. It is known that a plot of the ratio of reaction time (t) over the extent of reaction versus t has approximate slopes of 0.5 for a first-order reaction and 1.0 for a second-order reaction (Espenson, 1981). Our observed slope of 0.9 is again consistent with second-order but not first-order kinetics for the hairpin to duplex reaction.

Kinetic results for the hairpin to duplex reaction for the other AT oligomers of Chart I are also consistent only with second-order kinetics, and all rate constants are collected in Table I. There is no clear sequence dependence in the rate

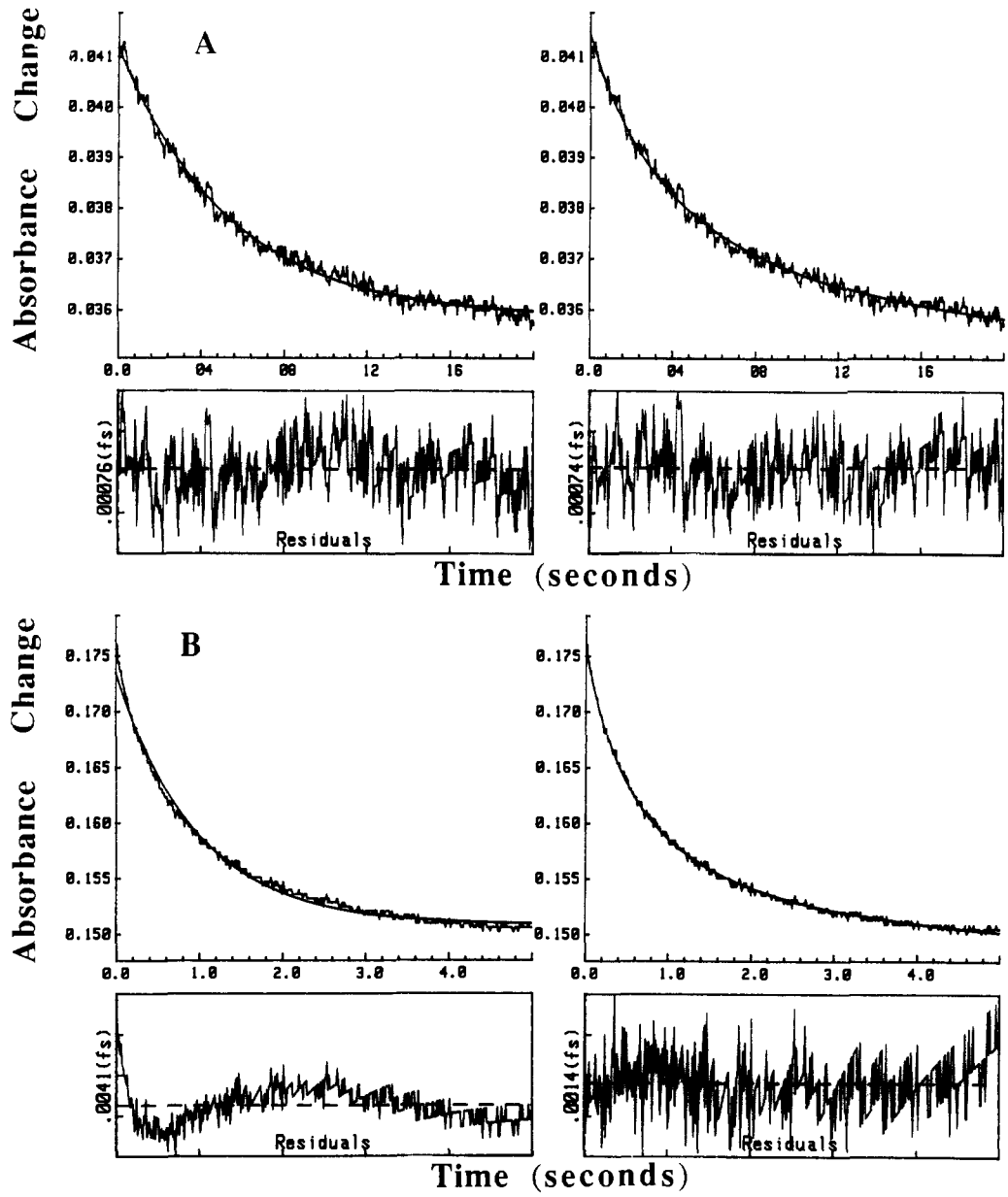

FIGURE 8: Kinetic traces for the hairpin to duplex reaction for $d(A_6T_6)$, determined by the stopped-flow (salt-jump) method at two different oligomer concentrations. At low concentration (A) the results are fitted reasonably well by both first-order (left side) and second-order (right side) functions. At higher concentration (B), the signal to noise is improved, and the second-order fit (right side) is clearly superior to the first-order fit (left side). The experiments were conducted at 23 °C by mixing $d(A_6T_6)$ in PIPES with no added salt with PIPES containing 0.4 M NaCl. The concentration in (A) was 1.08×10^{-5} M and the concentration in (B) was 7.58×10^{-5} M.

constants. The rate constants for $d(A_6T_6)$, $d(A_3T_3)_2$, and $d(A_2T_2)_3$ fall between 20×10^4 and 30×10^4 M^{-1} s^{-1} (±20%). The value for $d(T_6A_6)$ is slightly above this range, and the rate constant for $d(AT)_6$ is significantly larger than those for the other oligomers. These kinetics results provide conclusive evidence that the thermal transitions of the oligomers of Chart I involve hairpin intermediates. Duplex formation for a similar non-self-complementary oligomer sequence containing non-alternating AT base pairs was ~30 times faster (second-order rate constants of 9×10^6 M^{-1} s^{-1}) than for the oligomers of Chart I (Table I) (Tanious and Wilson, unpublished results). The rate constant for the non-self-complementary AT oligomer is in excellent agreement with kinetics results for duplex formation with a similar sequence [$d(CA_5G)$·$d(CT_5G)$] by Nelson and Tinoco (1982). The reaction of oligomers that cannot form hairpins involves nucleation of base pairing between the single strands and subsequent rate-limiting completion of base pairing to give the duplex [cf. Cantor and Schimmel (1980) and Nelson and Tinoco (1982)]. With oligomers that form hairpin intermediates during their pathway to the duplex, partial or complete opening of the hairpin becomes the rate-determining step (see Discussion).

In order to obtain more detailed mechanistic information on the hairpin to duplex reaction, the effects of temperature and ionic strength on the transition for the $d(A_6T_6)$ oligomer were evaluated. The boundary conditions for the temperature range that can be covered are limited by the temperatures of the duplex to hairpin transition in the two salt concentrations used in the salt-jump experiment. The temperature must be above the duplex to hairpin transition point in the low-salt buffer and below the duplex to hairpin transition temperature in the higher salt concentration buffer obtained after mixing. An Arrhenius plot (not shown) of results obtained on mixing oligomer in PIPES with PIPES containing 0.4 M NaCl was linear and yielded an activation energy of 31 kcal/mol. The activation energy for duplex formation from denatured strands is near zero (Nelson & Tinoco, 1982). The effect of salt concentration was evaluated by mixing the oligomer in 0.02

Table I: T_m Values for the Duplex to Denatured-Strand Equilibrium and the Rate Constant for Hairpin to Duplex Transition

oligomers	T_m (°C)[a]	$k \times 10^{-4}$ (M^{-1} s^{-1})[b]
Dickerson	56.2	[c]
$d(A_6T_6)$	41.2	29.9
$d(A_3T_3)_2$	37.2	20.2
$d(A_2T_2)_3$	33.8	31.2
$d(AT)_6$	30.1	51.7
$d(T_6A_6)$	30.9	34.1
$d(A_6T_6)$[d]	37.2	15.2
$d(A_6T_6)$[e]	32.6	5.4

[a] Determined at a total oligomer strand concentration of 1.3×10^{-5} M in PIPES buffer with 0.4 M NaCl. [b] The second-order rate constants were obtained by the salt-jump, stopped-flow method. The measurements were made at 20 °C in PIPES buffer with 0.4 M NaCl (mixing the oligomer in PIPES with PIPES containing 0.8 M NaCl), and the error in k is approximately ±20%. The molar units in the rate constant refer to oligomer strand molarities. [c] The hairpin to duplex reaction for this oligomer is too slow to be accurately followed with stopped-flow techniques. [d] These measurements were made at 20 °C in PIPES with 0.2 M NaCl (mixing the oligomer in PIPES with PIPES containing 0.4 M NaCl). [e] These measurements were made at 20 °C in PIPES with 0.1 M NaCl (mixing the oligomer in PIPES with PIPES containing 0.2 M NaCl).

M Na^+ buffer with buffers containing 0.2, 0.4, and 0.8 M Na^+ at 20 °C (Table I). As can be seen, the second-order rate constant increases significantly as the ionic strength increases.

Discussion

Because of the potential biological importance of the duplex-cruciform/hairpin equilibrium and the interesting and diverse properties of AT-containing DNA sequences, we have carried out a systematic study on the conformational transitions of dodecamers with varying AT base pair sequences (Chart I). The oligomers allow for several interesting comparisons: (i) increasing numbers of nonalternating AT base pairs from none to two to three and six, (ii) reverse sequences $d(A_6T_6)$ and $d(T_6A_6)$, and (iii) different possible arrangements of A and T base pairs at the 5′ and 3′ ends of the loop in hairpin conformations. It is now well established that self-complementary oligomers with AT central regions can have hairpin intermediates in their thermal transitions depending on the solution conditions (Scheffler et al., 1968, 1970; Cantor & Schimmel, 1980; Marky et al., 1983; Xodo et al., 1988a,b), and the results presented here indicate that the melting transitions for the oligomers of Chart I must be described in terms of the three possible species: duplex, hairpin, and denatured strand. This information is summarized in a qualitative way in Figure 9, which describes the transitions and regions of conformational stability for $d(A_6T_6)$ as an example. Since DNA charge densities depend more on conformation than sequence (Cantor & Schimmel, 1980), a diagram of similar shape would be obtained for all of the oligomers of Chart I but with the T_m values displaced. At low sodium ion concentrations and 0 °C in Figure 9, the duplex is the stable species. As the temperature is increased, at low ionic strength a duplex to hairpin transition occurs, and over an intermediate temperature range the hairpin is the most stable conformation. At higher temperature a hairpin to denatured-strand transition occurs. As the salt concentration is increased, the duplex remains stable at low temperature, but above a critical salt concentration there is no temperature at which the hairpin is stable, and under these conditions, only a duplex to denatured-strand transition is observed as the temperature is increased. It should be noted, however, that a hairpin can still occur as a transient intermediate in the denaturation reaction.

There are three clear criteria that establish the hairpin as an intermediate in the thermal transitions of the oligomers of

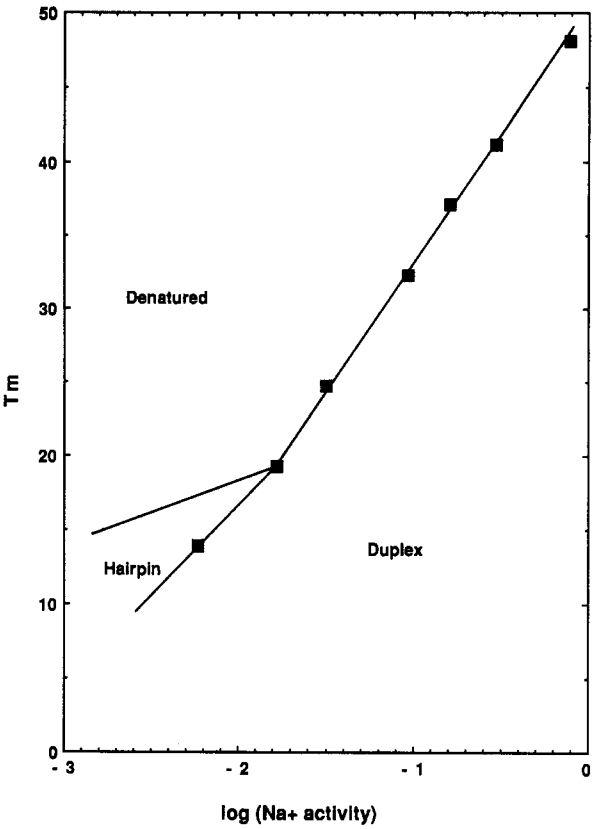

FIGURE 9: Hypothetical conformational-stability diagram for the duplex, hairpin, and denatured states of $d(A_6T_6)$.

Chart I and support the conclusions summarized in Figure 9: (i) The oligomers exhibit biphasic melting curves at low salt concentration with a sharp transition at low temperature followed by a broad transition at higher temperature. Non-self-complementary oligomers, such as $(dA)_n \cdot (dT)_n$, do not exhibit such biphasic transitions (Scheffler et al., 1968, 1970; Cantor & Schimmel, 1980; Marky et al., 1983; Xodo et al., 1988a,b; Tanious and Wilson, unpublished results). The transitions for the self-complementary oligomers become monophasic and similar to the thermal transitions for non-self-complementary oligomers at high salt concentrations where only the denatured-strand–duplex equilibrium is observed (Figures 1 and 9). (ii) CD spectra as a function of temperature at low salt concentration do not have isoelliptic points, and in the 270-nm spectral range they first increase and then decrease in molar ellipicity as the temperature is increased (Figure 3). (iii) The kinetics of duplex formation with a hairpin intermediate are much slower and the energy of activation is much higher relative to those of duplex formation for similar non-self-complementary oligomers that cannot form hairpins (Table I; Nelson & Tinoco, 1982; Tanious and Wilson, unpublished results).

The transitions for the alternating oligomer $d(AT)_6$ (Figure 1D) are displaced to significantly lower temperature relative to those of $d(A_6T_6)$, and at low temperature and salt concentration only the hairpin to denatured-strand equilibrium is observed for $d(AT)_6$. The sequences $d(A_3T_3)_2$ (Figure 1B) and $d(A_2T_2)_3$ (Figure 1C) have intermediate properties, but both show the sharp duplex to hairpin conformational transition even at the lowest ionic strength, and their mobilities at low temperature are more similar to those of $d(A_6T_6)$ than to those of $d(AT)_6$ (Figure 7). Qualitative analysis of CD spectra for $d(A_2T_2)_3$ and $d(A_3T_3)_2$ (Figure 3), relative to those of $d(A_6T_6)$ and the Dickerson sequence, indicates that both have spectra which are closer to the B-form type than to the

unusual spectra for $d(A_6T_6)$. This agrees with results by Crothers and co-workers (Haran & Crothers, 1989; Nadeau & Crothers, 1989), which indicate that four or more consecutive nonalternating AT pairs are needed to switch from B-type to the unusual conformation which promotes helix curvature.

The low-temperature CD spectra of $d(A_6T_6)$ and $d(T_6A_6)$ in the duplex state are similar but show small differences. Raman bands associated with 600–800-cm^{-1} sugar–base vibrations also have small intensity differences at 4 °C. These bands may be more sensitive to bound water than the higher frequency modes, which do not display detectable differences. At room temperature, higher thermal fluctuations may randomize any differences in water bound to the two duplexes, and at 25 °C no differences are observed for the two sequences. The global conformations of $d(T_6A_6)$ and $d(A_6T_6)$ are, thus, clearly quite similar to each other and different from the average B-form conformation. The $d(T_6A_6)$ sequence is significantly less stable than $d(A_6T_6)$, however, and converts to the hairpin conformation at lower temperatures than $d(A_6T_6)$. The duplex to hairpin transition for $d(T_6A_6)$ could be facilitated by two factors: (i) the lower stacking free energy of TpA versus ApT DNA sequences (Yoon et al., 1988; Klug et al., 1979) and (ii) the enhanced stability of DNA hairpin loops with 5′-pyrimidine and 3′-purine bases in the loop relative to the stability of the reverse sequence (Haasnoot et al., 1986, 1987). The combination of decreased duplex and enhanced hairpin stability could account for the lower free energy and T_m of $d(T_6A_6)$ relative to $d(A_6T_6)$.

It may also be worth noting that the two major inverted repeat sequences in plasmid pBR322 which form cruciforms under physiological supercoil tension (Lilley, 1981) or during a melting transition (McCampbell et al., 1989) have a d(TpA) step at the stem–loop junction. The presence or absence of this sequence at a junction may be an element in determining why some inverted repeats form cruciforms readily while others do not.

The rates for the hairpin to duplex transition are second order and are larger for the AT oligomers of Chart I (Table I) than for similar oligomers with terminal GC base pairs [Xodo et al. (1988a,b) and Figure 8]. These results explain the electrophoresis separation for the hairpin and duplex species of the Dickerson and d(GCATATATATGC) sequences and the observation of only a single band for the AT oligomers (Figure 7). Baldwin and co-workers (Scheffler et al., 1968) observed that the hairpin to duplex conversion for alternating AT oligonucleotides could be fitted with a single first-order rate constant. They did, however, find that the apparent first-order rate constant depended on the oligomer concentration, suggesting that the reaction was more complex than a simple first-order process. Our results provide an explanation for these observations. First, the reaction is clearly second order. It is well-known that the distinctions between first- and second-order reactions are quite difficult to distinguish by a simple fitting procedure and require data of very high signal to noise for the distinction to be made (Espenson, 1981). A textbook example of this problem is shown in Figure 8. Although the second-order fit is slightly better than the first-order fit at low concentration, the difference is not convincing. At the higher concentration with improved signal to noise, the second-order fit is clearly better than a first-order fit to the data. The concentration dependence and extent of reaction plots discussed earlier unequivocally define the hairpin to duplex reaction as second order.

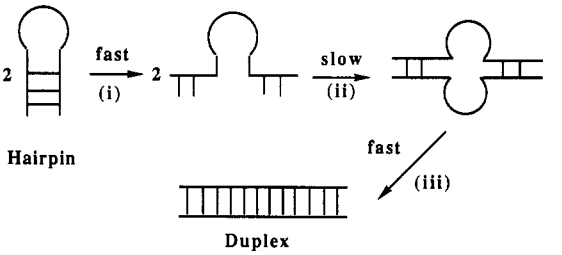

FIGURE 10: Cartoon for the proposed mechanism for the hairpin to duplex transition in the AT oligomers of Chart I.

The observed second-order kinetics suggests a mechanism for the hairpin to duplex reaction which involves two oligomer chains coming together in the transition state for the rate-determining step (Figure 10). Two additional pieces of information help to elucidate the mechanism for the transition: (i) the reaction rate constant increases with an increase in ionic strength, and (ii) the activation energy is approximately 30 kcal/mol. The salt dependence suggests that two anionic chains are brought together in the transition state to give a species of higher charge density than the reactants. Increasing ionic strength would thus increase the rate of reaction as observed. The low energy of activation suggests that a small number of base pairs at the ends of each hairpin are opened as the transition state is formed. A mechanism involving complete chain opening of the hairpin before formation of the duplex would result in a large energy of activation and a transition state of lower charge density than the hairpin. Increasing ionic strength would decrease the rate in such a mechanism.

A mechanism that is consistent with all of our results, shown in Figure 10, involves the following steps: (i) the terminal base pairs of two hairpin molecules are opened by thermal fraying, (ii) the two open species collide in such a way that a cruciform-type intermediate forms with higher charge density than the separated hairpins, and (iii) the bimolecular intermediate falls apart or intermolecular base pairing migrates to produce a duplex. NMR studies with oligomers with terminal AT base pairs have shown significant terminal fraying (Patel, 1984; Jones et al., 1988; Celda et al., 1989). This suggests that step i is very fast and reaches a preequilibrium. Bimolecular process ii requires two hairpins with open terminal base pairs to collide in an orientation that allows cruciform formation and is the rate-limiting step. Step ii is ionic strength dependent since the cruciform has a higher charge density than the separated hairpins. Step iii involves conversion of the unstable intermediate to product and is fast relative to step ii. All of the oligomers of Chart I have similar ionic strength dependent second-order reactions, suggesting that the mechanism is general for these pure AT sequence oligomers. The transition from duplex to hairpin for oligomers with terminal base GC base pairs is much slower and may involve an open-chain transition state (Xodo et al., 1988b).

It is well-known that cruciform/hairpin conformations occur in critical control regions of DNA sequences (Lilley et al., 1987). We have shown here that AT sequences of exactly the same size and composition have significantly different conformations, stabilities, and hairpin-forming tendencies. These results provide a microscopic look at the influence of sequence on hairpin formation in DNA and indicate that both sequence and composition are critical factors. These studies also expand our appreciation and understanding of the interesting and diverse properties of AT sequences in DNA.

Supplementary Material Available

Three figures showing melting curves in different salt concentration buffers for $d(A_3T_3)_2$, $d(A_2T_2)_3$, $d(AT)_6$, and $d(T_6A_6)$ (panels B–E of Figure 1, respectively), circular dichroism spectra for $d(A_3T_3)_2$, $d(A_2T_2)_3$, $d(AT)_6$, and $d(T_6A_6)$ (panels C–F of Figure 3, respectively), and Raman spectra for $d(A_6T_6)$ and $d(T_6A_6)$ and difference Raman spectrum for $d(A_6T_6)$ minus $d(T_6A_6)$ (Figure 6) (10 pages). Ordering information is given on any current masthead page.

References

Arnott, S. (1975) *Nucleic Acids Res. 2*, 1493–1502.

Blackburn, M., & Gait, M. (1990) *Nucleic Acids in Chemistry and Biology*, IRL Press Ltd., Oxford (in press).

Blommers, M. J. J., Haasnoot, C. A. G., & Hilbers, C. W. (1987) *Struct. Dyn. Polym. 133*, 78–79.

Bresloff, J. L., & Crothers, D. M. (1981) *Biochemistry 20*, 3547–3553.

Burkoff, A. M., & Tullius, T. D. (1987) *Cell 48*, 935–943.

Cantor, C. R., & Schimmel, P. R. (1980) *Biophysical Chemistry*, W. H. Freeman, San Francisco.

Celda, B., Widmer, H., Leupin, W., Chazin, W. J., & Denny, W. A. (1989) *Biochemistry 28*, 1462–1471.

Chaires, J. B. (1983) *Biochemistry 22*, 4204–4211.

Chen, J.-H., Churchill, M. E. A., Tullius, T. D., Kallenbach, N. R., & Seeman, N. C. (1988a) *Biochemistry 27*, 6032–6038.

Chen, J.-H., Seeman, N. C., & Kallenbach, N. R. (1988b) *Nucleic Acids Res. 16*, 6803–6812.

Coll, M., Frederick, C. A., Wang, A. H.-J., & Rich, A. (1987) *Proc. Natl. Acad. Sci. U.S.A. 84*, 8385–8389.

Dickerson, R. E., Drew, H. R., Conner, B. N., Wing, R. M., Fratini, A. V., & Kopka, M. L. (1982) *Science 216*, 475–485.

Diekmann, S. (1987) in *Nucleic Acids and Molecular Biology* (Eckstein, F., & Lilley, D., Eds.) Vol. I, pp 138–156, Springer-Verlag, Berlin.

DiGabriele, A. D., Sanderson, M. R., & Steitz, T. A. (1989) *Proc. Natl. Acad. Sci. U.S.A. 86*, 1816–1820.

Edmondson, S. D., & Johnson, C. R., Jr. (1985) *Biopolymers 24*, 825–841.

Espenson, J. H. (1981) *Chemical Kinetics and Reaction Mechanisms*, McGraw-Hill, New York.

Frank, R., & Koster, H. (1979) *Nucleic Acids Res. 6*, 2069–2087.

Gupta, G., Sarma, M. H., & Sarma, R. H. (1988) *Biochemistry 27*, 7909–7919.

Haasnoot, C. A. G., Hilbers, C. W., van der Marel, G. A., van Boom, J. H., Singh, U. C., Pattabiraman, N., & Kollman, P. A. (1986) *J. Biomol. Struct. Dyn. 3*, 739–1102.

Hagerman, P. J. (1986) *Nature 321*, 449–450.

Hanvey, J. C., Shimizu, M., & Wells, R. D. (1988) *Proc. Natl. Acad. Sci. U.S.A. 28*, 6292–6296.

Haran, T. E., & Crothers, D. M. (1989) *Biochemistry 28*, 2763–2767.

Htun, H., & Dahlberg, J. E. (1988) *Science 241*, 1791–1796.

Jones, R. L., Zon, G., Krishnamoorthy, C. R., & Wilson, W. D. (1986) *Biochemistry 25*, 7431–7439.

Jones, R. L., Scott, E. V., Marzilli, L. G., & Wilson, W. D. (1988) *Biochemistry 27*, 6021–6026.

Klug, A., Jack, A., Viswamitra, M. A., Kennard, O., Shakked, Z., & Steitz, T. A. (1979) *J. Mol. Biol. 131*, 669–680.

Lee, J. S., Woodsworth, M. L., Latimer, L. P., & Morgan, A. R. (1984) *Nucleic Acids Res. 12*, 6603.

Lilley, D. M. J. (1980) *Proc. Natl. Acad. Sci. U.S.A. 77*, 6468–6472.

Lilley, D. M. J., Sullivan, K. M., & Murchie, A. (1987) in *Nucleic Acids and Molecular Biology* (Eckstein, F., & Lilley, D., Eds.) Vol. I, pp 126–137, Springer-Verlag, Berlin.

Lyamichev, V. I., Mirkin, S. M., & Frank-Kamenetskii, M. D. (1986) *J. Biomol. Struct. Dyn. 3*, 667–669.

Maniatis, T., Jeffrey, A., & van de Sande, H. (1975) *Biochemistry 14*, 3787–3794.

Marky, L. A., Curry, J., & Breslauer, K. (1985) in *Molecular Basis of Cancer* (Rein, R., Ed.) pp 155–173, Alan R. Liss, New York.

Marky, L. A., Blumenfeld, K. S., Kozlowski, S., & Breslauer, K. (1983) *Biopolymers 22*, 1247–1257.

McCampbell, C. R., & Wartell, R. M. (1989) *Biopolymers 28*, 1745–1758.

Moser, H. E., & Dervan, P. B. (1987) *Science 238*, 645–650.

Nadeau, J. G., & Crothers, D. M. (1989) *Proc. Natl. Acad. Sci. U.S.A. 86*, 2622–2626.

Nelson, J. W., & Tinoco, I. (1982) *Biochemistry 21*, 5289–5294.

Nelson, H. C. M., Finch, J. T., Luisi, B. F., & Klug, A. (1987) *Nature 330*, 221–226.

Oliver, A. L., Wartell, R. M., & Ratliff, R. L. (1977) *Biopolymers 16*, 1115–1123.

Patapoff, T. W., Thomas, G. A., Wang, Y., & Peticolas, W. L. (1988) *Biopolymers 27*, 493–507.

Patel, D. J. (1984) *Biochemistry 13*, 2396–2402.

Patel, D. J., Kozlowski, S. A., Marky, L. A., Broka, C., Rice, J., Itakura, K., & Breslauer, K. J. (1982) *Biochemistry 21*, 428–436.

Peticolas, W. L., Kvbasek, W. L., Thomas, G. A., & Tsuboi, M. (1987) *Biological Applications of Raman Spectroscopy* (Spiro, T. G., Ed.) Vol. 1, pp 81–133, Wiley, New York.

Petrillo, M. L., Newton, C. J., Cunningham, R. P., Ma, R.-I., & Kallenbach, N. R. (1988) *Biopolymers 27*, 1337–1352.

Saenger, W. (1984) *Principles of Nucleic Acids Structure*, Springer-Verlag, New York.

Sarma, M. H., Gupta, G., & Sarma, R. H. (1988) *Biochemistry 27*, 3423–3432.

Scheffler, I. E., Elson, E. L., & Baldwin, R. L. (1968) *J. Mol. Biol. 36*, 291–304.

Scheffler, I. E., Elson, E. L., & Baldwin, R. L. (1970) *J. Mol. Biol. 48*, 145–171.

Strum, J. (1982) *Biopolymers 21*, 1189–1206.

Thomas, G. A., & Peticolas, W. L. (1983) *J. Am. Chem. Soc. 105*, 986–992.

Thomas, G. J., Jr. (1987) in *Biological Applications of Raman Spectroscopy* (Spiro, T. G., Ed.) Vol. 1, pp 135–203, Wiley, New York.

Trifonov, E. N. (1985) *CRC Crit. Rev. Biochem. 19*, 89–106.

Viswamitra, M. A., Shakked, Z., Jones, P. G., Sheldrick, G. M., Salisbury, S. A., & Kennard, O. (1982) *Biopolymers 21*, 513–533.

Wang, A. H.-J., Quigley, G. J., Kolpak, F. L., Crawford, J. L., van Boom, J. H., van der Marel, G., & Rich, A. (1979) *Nature 282*, 680–686.

Wartell, R. M., & Harrell, J. T. (1986) *Biochemistry 25*, 2664–2671.

Wells, R. D., & Larson, J. E. (1970) *J. Mol. Biol. 49*, 319–342.

Wells, R. D., & Harvey, S. C. (1987) *Unusual DNA Structures*, Springer, New York.

Wemmer, D. E., Hare, D. R., & Reid, B. R. (1985) *Nucleic Acids Res. 13*, 3755–3771.

Wilson, W. D., Wang, Y.-H., Krishnamoorthy, C. R., & Smith, J. C. (1985a) *Biochemistry 24*, 3991–3999.

Wilson, W. D., Wang, Y.-H., Kusuma, S., Chandrasekaran, S., Yang, N. C., & Boykin, D. W. (1985b) *J. Am. Chem. Soc. 107*, 4989-4995.
Wilson, W. D., Wang, Y.-H., Krishnamoorthy, C. R., & Smith, J. C. (1986) *Chem.-Biol. Interact. 56*, 41-56.
Wilson, W. D., Zuo, E. T., Jones, R. L., Zon, G., & Baumstark, B. R. (1987) *Nucleic Acids Res. 15*, 105-118.
Wu, H.-M., & Crothers, D. S. (1984) *Nature 308*, 509-513.
Xodo, L. E., Manzini, G., Quadrifoglio, F., van der Marel, G. A., & van Boom, J. (1988a) *J. Biomol. Struct. Dyn. 6*, 139-152.
Xodo, L. E., Manzini, G., Quadrifoglio, F., van der Marel, G. A., & van Boom, J. (1988b) *Biochemistry 27*, 6321-6326.
Yoon, C., Prive, G. G., Goodsell, D. S., & Dickerson, R. E. (1988) *Proc. Natl. Acad. Sci. U.S.A. 85*, 6332-6336.

NMR Studies of an Exocyclic 1,N^2-Propanodeoxyguanosine Adduct (X) Located Opposite Deoxyadenosine (A) in DNA Duplexes at Basic pH: Simultaneous Partial Intercalation of X and A between Stacked Bases†

Michael Kouchakdjian,‡ Moises Eisenberg,§ David Live,∥ Edmund Marinelli,§ Arthur P. Grollman,*,§ and Dinshaw J. Patel*,‡

Department of Biochemistry and Molecular Biophysics, College of Physicians and Surgeons, Columbia University, New York, New York 10032, Department of Pharmacological Sciences, State University of New York at Stony Brook, Stony Brook, New York 11794, and Chemistry Department, Emory University, Atlanta, Georgia 30322

Received September 12, 1989; Revised Manuscript Received November 29, 1989

ABSTRACT: The NMR parameters for the 1,N^2-propanodeoxyguanosine (X) opposite deoxyadenosine positioned in the center of the complementary d(C1-A2-T3-G4-X5-G6-T7-A8-C9)·d(G10-T11-A12-C13-A14-C15-A16-T17-G18) X·A 9-mer duplex are pH dependent. A previous paper established protonated X5(syn)·A14(anti) pairing in the X·A 9-mer duplex at pH 5.8 [Kouchakdjian, M., Marinelli, E., Gao, X., Johnson, F., Grollman, A., & Patel, D. J. (1989) *Biochemistry 28*, 5647-5657]; this paper focuses on the pairing alignment at the lesion site at pH 8.9. The observed NOEs between specific exocyclic CH_2 protons and both the imino proton of G6 and the sugar H1′ protons of C13 and A14 establish that X5 is positioned toward the G6·C13 base pair with the exocyclic ring directed between C13 and A14 on the partner strand. The observed NOE between the H2 proton of A14 and the imino proton of G4, but not G6, establishes that A14 at the lesion site is directed toward the G4·C15 base pair. NOEs are detected between all exocyclic CH_2 protons of X5 and the H2 proton of A14, confirming that both X5 and A14 are directed toward the interior of the helix. The X5(anti)·A14(anti) alignment at pH 8.9 is accommodated within the helix with retention of Watson-Crick pairing at flanking G4·C15 and G6·C13 base pairs. The energy-minimized conformation of the (G4-X5-G6)·(C13-A14-C15) segment at pH 8.9 establishes that X5 and A14 are directed into the helix, partially stack on each other, and are not stabilized by intermolecular hydrogen bonds. The X5 base is partially intercalated between C13 and A14 on the unmodified strand, while A14 is partially intercalated between G4 and X5 on the modified strand. This results in a larger separation between the G4·C15 and G6·C13 base pairs flanking the lesion site in the basic pH conformation of the X·A 9-mer duplex. The midpoint of the transition between the protonated X5(syn)·A14(anti) and X5(anti)·A14(anti) conformations occurs at pH 7.6, establishing an unusually high pK_a for protonation of the A14 ring opposite the X5 exocyclic adduct site. Thus, the interplay between hydrophobic and hydrogen-bonding contributions modulated by pH defines the alignment of 1,N^2-propanodeoxyguanosine opposite deoxyadenosine in the interior of DNA helices.

There is currently very little known at the molecular level about structural features of nucleic acid exocyclic adducts important in mutagenesis and carcinogenesis (Shapiro, 1969; Singer & Grunberger, 1983; Singer & Bartsch, 1986; Basu & Essigmann, 1988). The formation of these adducts not only interferes with base-pairing regions in nucleic acid components but also induces substantial alterations in pK_a and hydrophobicity at the lesion site. There is a potential for local helix distortion at sites of exocyclic adduct formation, which may exert substantial effects on DNA replication and repair and lead ultimately to mutagenesis and carcinogenesis.

Exocyclic adducts may be generated through Michael addition of α,β-unsaturated carbonyl compounds to the N1 and N2 positions of deoxyguanosine followed by ring closure. Our studies have focused on the 1,N^2-propanodeoxyguanosine adduct **1** (Marinelli et al., 1990), which is a stable analogue of the adduct generated with acrolein but lacking the hydroxyl group (Chung et al., 1984). We have inserted exocyclic adduct **1** into DNA oligonucleotide duplexes in order to determine the structural and biological consequences of the additional ring in the adduct with the goal of elucidating the molecular basis of the mutagenic potential of exocyclic adducts.

Biological studies in vivo and in vitro have shown that upon replication, deoxyadenosine is incorporated preferentially opposite 1,N^2-propanodeoxyguanosine (Grollman, 1989).

† This research was supported by NIH CA-49982 to D.J.P. and NIH CA-47995 to A.P.G. NMR studies were conducted on instruments purchased with funds provided by the Robert Woods Johnson Jr. Charitable Trust and Matheson Foundation.
‡ Columbia University.
§ State University of New York at Stony Brook.
∥ Emory University.

0006-2960/90/0429-4456$02.50/0